(12)

College of Earth and Mineral Sciences

PENNSTATE

ANNUAL TECHNICAL REPORT

~~December 1990~~

OFFICE OF NAVAL RESEARCH

Contract NO. N0014-86-K-0133

POINT DEFECT EFFECTS ON HOT CORROSION OF ZIRCONIA-BASED COATINGS

R. Reidy, D-H. Kim, and G. Simkovich

Depart of Materials Science and Engineering
The Pennsylvania State University
University Park, Pennsylvania 16802

PENN STATE
College of Earth and Mineral Sciences

Undergraduate Majors

Ceramic Science and Engineering, Fuel Science, Metals Science and Engineering, Polymer Science; Mineral Economics; Mining Engineering, Petroleum and Natural Gas Engineering; Earth Sciences, Geosciences; Geography; Meteorology.

Graduate Programs and Fields of Research

Ceramic Science and Engineering, Fuel Science, Metals Science and Engineering, Polymer Science; Mineral Economics; Mining Engineering, Mineral Processing, Petroleum and Natural Gas Engineering;
Geochemistry and Mineralogy, Geology, Geophysics; Geography; Meteorology.

Universitywide Interdisciplinary Graduate Programs Involving EMS Faculty and Students

Earth Sciences, Ecology, Environmental Pollution Control Engineering, Mineral Engineering Management, Solid State Science.

Associate Degree Programs

Metallurgical Engineering Technology (Shenango Valley Campus).

Interdisciplinary Research Groups Centered in the College

C. Drew Stahl Center for Advanced Oil Recovery, Center for Advanced Materials, Coal Research Section, Earth System Science Center, Mining and Mineral Resources Research Institute, Ore Deposits Research Group.

Analytical and Characterization Laboratories (Mineral Constitution Laboratories)

Services available include: classical chemical analysis of metals and silicate and carbonate rocks; X-ray diffraction and fluorescence; electron microscopy and diffraction; electron microprobe analysis; atomic absorption analysis; spectrochemical analysis; surface analysis by secondary ion mass spectrometry (SIMS); and scanning electron microscopy (SEM).

U.Ed. 87-1027
Produced by the Penn State Department of Publications

SECURITY CLASSIFICATION OF THIS PAGE

REPORT DOCUMENTATION PAGE

1a. REPORT SECURITY CLASSIFICATION	1b. RESTRICTIVE MARKINGS
2a. SECURITY CLASSIFICATION AUTHORITY	3. DISTRIBUTION/AVAILABILITY OF REPORT
2b. DECLASSIFICATION/DOWNGRADING SCHEDULE	
4. PERFORMING ORGANIZATION REPORT NUMBER(S) Metallurgy Program, 209 Steidle Bldg.	5. MONITORING ORGANIZATION REPORT NUMBER(S)
6a. NAME OF PERFORMING ORGANIZATION Metallurgy Program 6b. OFFICE SYMBOL (If applicable)	7a. NAME OF MONITORING ORGANIZATION Metallurgy Branch
6c. ADDRESS (City, State and ZIP Code) 209 Steidle Bldg. The Pennsylvania State University University Park, PA 16802	7b. ADDRESS (City, State and ZIP Code) Office of Naval Research Arlington, VA 22217
8a. NAME OF FUNDING/SPONSORING ORGANIZATION Metallurgy Branch 8b. OFFICE SYMBOL (If applicable)	9. PROCUREMENT INSTRUMENT IDENTIFICATION NUMBER N0014-86-K-0133 (contract number)
8c. ADDRESS (City, State and ZIP Code) Office of Naval Research Arlington, VA 22217	10. SOURCE OF FUNDING NOS. PROGRAM ELEMENT NO. / PROJECT NO. / TASK NO. / WORK UNIT NO.
11. TITLE (Include Security Classification) Point Defect Effects on Hot Corrosion of Zirconia-based Coatings	
12. PERSONAL AUTHOR(S) R. Reidy, D-H. Kim, and G. Simkovich	
13a. TYPE OF REPORT Annual Technical Report	13b. TIME COVERED FROM 1-90 to 1-91
14. DATE OF REPORT (Yr., Mo., Day) 1991-23-1	15. PAGE COUNT
16. SUPPLEMENTARY NOTATION	

17. COSATI CODES			18. SUBJECT TERMS (Continue on reverse if necessary and identify by block number)
FIELD	GROUP	SUB. GR.	

19. ABSTRACT (Continue on reverse if necessary and identify by block number)

Thermal barrier coatings are vulnerable to certain types of hot corrosion: sulfidation and vanadic attack. Stabilized zirconia, an often used thermal barrier coating, is degraded by dissolution of the stabilizing component (e.g. Y_2O_3). To obtain the dissolution of the stabilizing components, mass transport in the coating must occur. The presence of point defects in a crystalline solid greatly affect the transport properties in that solid. The nature and concentration of these defects can be altered which, in turn, can impart large changes in the transport properties of a material (eg. ionic conductivity and diffusion). In this study, we are determining the defect structures of yttria and ceria-stabilized zirconium oxides. Using electrical conductivity measurements, the activation energies of yttria-stabilized zirconia have been examined as a function of frequency, composition, and oxygen activity.
(see back)

20. DISTRIBUTION/AVAILABILITY OF ABSTRACT UNCLASSIFIED/UNLIMITED ☐ SAME AS RPT ☐ DTIC USERS ☐	21 ABSTRACT SECURITY CLASSIFICATION
22a. NAME OF RESPONSIBLE INDIVIDUAL	22b TELEPHONE NUMBER (Include Area Code) / 22c. OFFICE SYMBOL

DD FORM 1473, 83 APR EDITION OF 1 JAN 73 IS OBSOLETE.

SECURITY CLASSIFICATION OF THIS PAGE

Conductivity measurements on ceria-stabilized zirconia have shown anomalous results. At low oxygen activities, ZrO_2–CeO_2 samples did not reach equilibrium. The cause for this phenomenon has yet to be determined.

The transport properties of molten Na_2SO_4 have been investigated to aid to further understanding hot corrosion processes at 1173 K. An A.C. impedance technique for the total electrical conductivity, the potentiostatic polarization method for ionic transport numbers, and the steady state polarization method of Wagner and Hebb for the electronic conductivity were employed as a function of Na_2O activity in the melt by controlling the gas atmosphere.

ABSTRACT

Thermal barrier coatings are vulnerable to certain types of hot corrosion: sulfidation and vanadic attack. Stabilized zirconia, an often used thermal barrier coating, is degraded by dissolution of the stabilizing component (e.g. Y_2O_3). To obtain the dissolution of the stabilizing components, mass transport in the coating must occur. The presence of point defects in a crystalline solid greatly affect the transport properties in that solid. The nature and concentration of these defects can be altered which, in turn, can impart large changes in the transport properties of a material (eg. ionic conductivity and diffusion). In this study, we are determining the defect structures of yttria and ceria-stabilized zirconium oxides. Using electrical conductivity measurements, the activation energies of yttria-stabilized zirconia have been examined as a function of frequency, composition, and oxygen activity. Conductivity measurements on ceria-stabilized zirconia have shown anomalous results. At low oxygen activities, ZrO_2-CeO_2 samples did not reach equilibrium. The cause for this phenomenon has yet to be determined.

The transport properties of molten Na_2SO_4 have been investigated to aid to further understanding hot corrosion processes at 1173 K. An A.C. impedance technique for the total electrical conductivity, the potentiostatic polarization method for ionic transport numbers, and the steady state polarization method of Wagner and Hebb for the electronic conductivity were employed as a function of Na_2O activity in the melt by controlling the gas atmosphere.

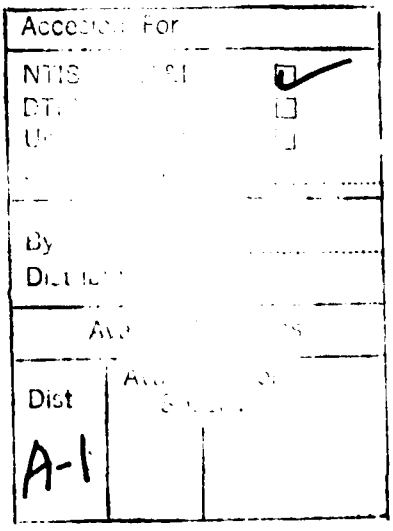

INTRODUCTION

Due to the severity of their operating environments, marine turbines are subject to a variety of corrosive mechanisms. One of the most formidable forms of attack is hot corrosion, a chemical interaction leading to a breakdown of a protective oxide scale.(1) There are two dominant types of hot corrosion: sulfidation and vanadium attack.

In sulfidation, NaCl reacts with sulfur found in the fuel to form Na_2SO_4. The sodium sulfate reacts with the protective oxide scale resulting in scale failure.(1,2) A large body of work details the roles of Na_2SO_4 and NaCl in the destruction of the oxide scale.(1-8)

Vanadium enters the turbine as a fuel impurity in organic and inorganic forms. These compounds react with oxygen to form oxides (VO, VO_2, VO_3, and V_2O_5) and hydroxides ($V_2O_7H_4$, $VO(OH)_3$, and $VO_2(OH)_2$).(9) These gases either condense onto the turbine blades and react with sodium compounds to form sodium vanadates as in equations 1-3),

$$2VO(OH)_3(g) = V_2O_5(l) + 3H_2O(g) \quad 1)$$

$$V_2O_5(g) = V_2O_5(l) \quad 2)$$

$$V_2O_5(l) + Na_2O(l) = 2NaVO_3(l) \quad 3)$$

or react with sodium compounds in the gas phase forming sodium vanadates which condense onto the turbine blades as in equation 4).

$$VO(OH)_3(g) + NaOH(g) = NaVO_3(l) + 2H_2O(g) \quad 4)$$

In addition to Na_2SO_4, Luthra and Spacil found both V_2O_5 and $NaVO_3$ in the condensate; therefore, it is difficult to determine which compound is more destructive to the oxide.(9) Further, one can not ignore the effects of Na_2SO_4 in a separate or combined attack on the oxide scale.

The mechanisms by which the sulfur or vanadium compounds disrupt protective oxide scales of nickel-based superalloys in marine turbine hot zones are detailed in several literature surveys.(1,7,10) Bornstein and DeCrescente (2) and Jones (8) describe a general mechanism referred to as the salt fluxing or acid-base reaction model. In sulfidation, Bornstein explains that the oxide scales are insoluble in stoichiometric sodium sulfate, but due to the reaction,

$$\underset{\text{(molten salt)}}{Na_2SO_4(l)} = \underset{\text{(base)}}{Na_2O} + \underset{\text{(acid)}}{SO_3} \qquad 5)$$

the oxide may dissolve in the base as an anion or in the acid as a cation.(1) From the Lux-Flood theory (11), the activities of the acidic and basic components in the molten salt are fixed by the dissociation constant of the reversible reaction 5).(8) In vanadium attack, a similar dissolution mechanism utilizes the Lewis definition of acids (electron acceptors) and bases (electron donors). Jones describes the ability of vanadium pentoxide to behave as a Lewis acid and react with a protective oxide.(8)

$$\underset{\text{(base)}}{Y_2O_3(s)} + \underset{\text{(acid)}}{V_2O_5(l)} = \underset{\text{(salt)}}{2YVO_4(l)} \qquad 6)$$

This dissolution mechanism involves the transport of electrons from the stabilizing component to the corrosive V_2O_5. A greater understanding of this transport phenomenon could yield the ability to retard or halt this dissolution.

Defect Chemistry

Rarely in nature does one find a perfect crystal. Instead, a number of disruptions occur in the periodic array of atoms. There are four general types of structural imperfections: point defects, line defects, plane defects, and

volume defects.(12) In crystalline solids, the nature and concentration of point defects greatly affect transport properties.

The type and concentration of point defects in an oxide is often dependent on the temperature, pressure, and chemical potentials of the oxide components.(13) Atomic defects (vacancies, interstitials, impurities, or misplaced atoms) affect solid state diffusion and non-stoichiometry of compounds. Changes in these properties, in turn, alter reaction rates, ionic conductivities, and sintering rates. Electronic defects (electrons and electron holes) determine electrical conductivities as well as other properties.(14,15) Therefore, a detailed understanding of the point defect behavior of a compound would provide great insight or even allow one to predict the transport phenomena in that material. Additionally, one may alter the transport properties of a compound by changing the nature or concentration of the point defects within it.

The effects of point defects on hydrometallurgical processes, such as flotation and dissolution, have been the subject of many studies.(16) In lead sulfide (PbS) which shows p-type conduction at high S_2 partial pressures and n-type at low S_2 partial pressures, additions of Ag_2S impart more p-type behavior while Bi_2S_3 doping creates a larger n-type contribution.(17) When the reaction rate is controlled by the interfacial reaction, Simkovich and Wagner found that the dissolution rates in nitric acid of PbS containing Ag_2S are greater than both pure PbS and Bi_2S_3-doped PbS.(16) Similar effects of dopant-induced changes in dissolution rates in NiO (17) and ZnO (18) have been documented. Some alterations in the defect structure of a base material which result in changes in dissolution behavior are an increased concentration of electron holes in Li_2O-doped NiO (19) and an increase in zinc interstitials in Li_2O-doped ZnO (20). Simkovich and Wagner detail other systems and the mechanisms by which changes in defect concentration directly affect dissolution rates.(21-26)

Thermal Barrier Coatings

In recent years, efforts have been made to apply protective ceramic coatings to turbine blades to improve resistance to hot corrosion as well as to increase engine operating temperatures.(27-29) These higher operating temperatures are attained because these coatings have high melting points and low thermal conductivities, thus protecting the more temperature sensitive alloy beneath. These materials are referred to as thermal barrier coatings.

With additions of various stabilizers, zirconia has been used as a thermal barrier coating. Due to a relatively high coefficient of thermal expansion (as compared to other ceramics), ZrO_2 minimizes thermal expansion differences between metal substrate and coating. However, the primary reason for considering stabilized ZrO_2 as a thermal barrier coating is its resistance to many forms of corrosion.

Pure zirconium oxide is a polymorphic compound. Three different stable forms of zirconia exist: cubic (fluorite structure, 2370 - 2680°C), tetragonal (1170 - 2370°C), and monoclinic (below 1170°C).(30) The phase transition from tetragonal to monoclinic has caused considerable concern. Early studies have determined that the transformation is martensitic (31) and does not occur at a fixed temperature, but over a temperature range, and involves a large (about 9%) volume expansion. This volume increase causes cracking in the ZrO_2 when cooled below the transition; therefore, traditional cooling methods to below 1170°C can result in crumbling of the zirconia.

The addition of CaO, MgO, Y_2O_3, and CeO_2 to zirconia lowers the transition temperatures of both solid state phase transformations.(30) Stubican and Hellmann (32) have reviewed the binary oxide phase diagrams and have shown a partially stabilized form (a mixture of cubic and tetragonal or monoclinic phases) and a fully stabilized zirconia (cubic phase). Both the cubic and mixed phases are stable at room temperature.

Wagner demonstrated that stabilized zirconia contains oxygen ion vacancies.(33) In calcia-stabilized zirconia, Hund (34) discovered that calcium

and zirconium ions are distributed statistically in the cation sites while an oxygen vacancy concentration equal to the calcium dopant concentration provides electroneutrality. Using x-ray diffraction methods, Tien and Subbarao have determined similar defect behavior in other stabilized zirconias.(35) Other investigators have concluded that the defect structure and concentration are fixed by dopant content.(36-40) Alcock has found that the electronic defect structure of stabilized zirconia is affected by changes in atmosphere and temperature.(41)

The primary thrust of this work is to determine the effect of point defects on the mechanisms and transport properties involved in the hot corrosion of zirconia coatings. It is prudent to briefly review the recent efforts to study these mechanisms by other methods.(5,42,43) The sulfidation and vanadium attack studies by Jones and Williams (44,45) demonstrated that ZrO_2 is substantially more resistant to hot corrosion than the dopants, Y_2O_3, CeO_2, and HfO_2. In other work, Jones discusses the degradation of the coating with respect to the acid-base reaction model.(5) The V_2O_5 reacts with the Y_2O_3 in the zirconia and forms a yttrium vanadate (equation 5)). The removal of yttria destabilizes the zirconia allowing the more voluminous monoclinic phase to form and leading to surface cracking of the coating. As the protective scale is thermally cycled, the cracks propagate and extend into the coating causing spallation. This mechanism has been put forth by a number of other investigators.(46-48)

Also included in this report is a summary of recently completed work on transport properties in molten sodium sulfate which was in part supported by this contract. The transport properties of a Na_2SO_4 melt has been investigated to aid in further understanding hot corrosion processes at 1173 K. An A. C. impedance technique for the total electrical conductivity, the potentiostatic polarization method for ionic transport numbers, and the steady state polarization method of Wagner and Hebb for the electronic conductivity were carried out as a function of Na_2O activity in the melt by controlling the gas atmosphere.

EXPERIMENTAL

Electrical and Ionic Conductivity

The electrical conductivity will be measured by a digital bridge using a two-point probe or a four-wire technique. The conductivity measurements will be taken at a number of temperatures (700-1100°C) and oxygen partial pressures. In addition, an Arrhenius plot of conductivity and temperature can estimate the activation energy of conduction.(7) By definition, conductivity is the product of the charge, the concentration of charge carriers, and the mobilities of those carriers. In an electrical conductivity measurement, the carriers can be either electronic or ionic.

To isolate the ionic contribution, potentiostatic polarization techniques can estimate the ionic transport numbers (the fraction of the total conductivity which is carried by ions).(35,43)

anode		cathode
Pt	stabilized	Pt
$P_{O2}' < 1$ atm	ZrO_2	$P_{O2}'' = 1$ atm

$$\Delta G = \Delta G^\circ + RT \ln Q \qquad 6)$$

$$= (G^\circ_{MO} + RT \ln a_{MO}'') + (G^\circ_{O2} + RT/2 \ln a_{O2}') - (G^\circ_{MO} + RT \ln a_{MO}') - (G^\circ_{O2} + RT/2 \ln a_{O2}'') \qquad 7)$$

$$= RT \ln (a_{MO}''/a_{MO}') + RT/2 \ln (P_{O2}'/P_{O2}'') \qquad 8)$$

$$\Delta G = -nFE \qquad 9)$$

$$= -NFE = RT \ln (a_{MO}''/a_{MO}') + RT/2 \ln (P_{O2}'/P_{O2}'') \qquad 10)$$

therefore,

$$E = (RT/nF) \ln (a_{MO}'/a_{MO}'') + (RT/2nF) \ln (P_{O2}''/P_{O2}') \qquad 11)$$

Eq. 11 applies when all current is carried by ionic species or vacancies. However, if any electronic transport exists, then the right side of Eq. 11 must be multiplied by t_i, the ion transport number.

$$E = t_i \left[(RT/Nf) \ln (a_{MO}'/a_{MO}'') + (RT/2nF) \ln (P_{O2}''/P_{O2}')\right] \quad 12)$$

Although the metal oxide activities are not known, they can be assumed to be nearly equal in a small oxygen potential gradient. Consequently,

$$a_{MO}' \approx a_{MO}''$$

$$E = E_{meas} = t_i \left[(RT/2nF) \ln (P_{O2}''/P_{O2}')\right] \quad 13)$$

and

$$E = E_{max} = (RT/2nF) \ln (P_{O2}''/P_{O2}') \quad 14)$$

E_{max} is calculated from experimental conditions, and E_{meas} is the measured emf. The value of t_i is the ratio of these results.

$$t_i \approx E_{meas}/E_{max} \quad 15)$$

Wagner-Hebb Polarization Experiments

The electronic contributions will be determined by Wagner-Hebb type polarization method.(30-31) This cell can be schematically represented as:

(negative)		(positive)
Zr	Stabilized	inert
electrode	Zirconia	electrode

The appropriate choice of electrodes enables the suppression of either electronic or ionic migration.(51,52) The partial conductivity of the electronic species can be determined from the ratio of the current density and the potential gradient.(53,54) Under steady state conditions, Wagner has derived equations for the total electronic current through the polarization cell.

$$I_{elec} = I_e + I_\theta \quad 16)$$

$$= RTA/LF \{\sigma_\theta^\circ[1 - \exp(-EF/RT)]$$

$$+ \sigma_{\oplus}^{\circ}[\exp(EF/RT) - 1]\} \quad 17)$$

Dividing eq. 17) by [1 - exp(-EF/RT)] and rearranging yields:

$$I_{elec} \{RTA/LF [1 - \exp(-EF/RT)]^{-1}\} = \sigma_{\ominus}^{\circ} + \sigma_{\oplus}^{\circ}\exp(EF/RT) \quad 18)$$

Plotting the left side of eq. 18) versus exp(EF/RT), the resulting line has $\sigma_{\oplus}^{\circ}$as its slope and $\sigma_{\ominus}^{\circ}$ as its intercept.(53,54) These quantities combined with the total electrical conductivity allow determination of the electronic transport numbers.

RESULTS AND DISCUSSION

Materials

In order to accurately describe the point defect structure of a material, the effects of macroscopic flaws such as pores and cracks should be reduced or, if possible, eliminated. As stated earlier, most commercial zirconia powders that were available did not fully densify during sintering. After a number of attempts, only one commercial powder had the necessary purity and could be fully densified (achieve densities 95% of theoretical values). Samples fabricated from other powders gave unreliable results. In order to control densities, composition, and purity, powders were synthesized by coprecipitation reactions. Using a protocol adapted from the work by Ciftcioglu and Mayo (48), nano-crystalline powders were prepared. By controlling sintering temperatures and times, one should be able to fix grain size in samples. At present, such control has proved difficult. As was shown in Fig. 1, the electrical properties of these ultra-fine grained samples seemed very different from larger grained samples despite having the same composition. A coprecipitation procedure for CeO_2-ZrO_2 by Duh et al. (49) may also be adapted to yield nano-crystalline powders.

Electrical Measurements

Electrical conductivity measurements for 3 and 8 mole percent yttria-stabilized zirconia have provided some interesting results. As a function of temperature, conductivity behaved in accordance with the literature values (the activation energies were approximately 1 eV)(50)(Fig.2). However, as a function of oxygen activity, the results did not follow behavior described by other researchers. Previous work has found for a number of compositions in yttria-stabilized zirconia that oxygen does not significantly affect conductivity except at very low oxygen partial pressures.(50) Our results have shown conductivity to increase as a function of P_{02} although only slightly (Fig.3). This behavior has been reproduced in a number of experiments.

Conductivity measurements on ceria-stabilized zirconia have also shown anomalous results. At low oxygen activities, ZrO_2-CeO_2 samples did not reach equilibrium. After well over 100 hours, the electrical conductivity continued to increase with no hint of leveling off (Fig.4). The cause for this phenomenon has yet to be determined. However, high temperature x-ray diffraction studies are currently underway to discover the effect of these low oxygen activities on the ZrO_2-CeO_2 structure.

Na_2SO_4 Studies

A large thrust of this experimental program was to obtain the transport properties in the aggressive molten salt Na_2SO_4. Table I list such information obtained from this study. The total electrical conductivity determined by utilizing an A.C. impedance technique indicates that pure Na_2SO_4 melt had a somewhat low total conductivity as compared to most ionic melts.

The cationic transport numbers of a pure Na_2SO_4 melt were obtained by utilizing the potentiostatic polarization technique. The results indicate that a pure Na_2SO_4 melt is a cationic conductor over a wide range of Na_2O activities

at 1173 K. From the above results, the diffusivity of cations, one of the important kinetic parameters, can be estimated as 8.1 x 10^{-6} cm^2/sec.

The Wagner-Hebb type polarization experiments provided the electron and electron hole conductivities in a pure Na_2SO_4 melt at 1173 K. From these measurements along with total electrical conductivity data, the transport numbers of electrons, t_e, and electron holes, $t_\oplus$, were calculated. Such experimental investigations show that the electronic conduction occurs primarily via the transport of electrons as indicated in Table I.

Table I

Transport Properties of a Pure Na_2SO_4 Melt

Ionic Transport Properties	Electronic Transport Properties
σ_{total} = 0.232 $(\Omega\text{-cm})^{-1}$	σ_e = 1.638 x 10^{-3} $(\Omega\text{-cm})^{-1}$
t_{Na^+} = 0.9838	$\sigma_\oplus$ = 1.337 x 10^{-5} $(\Omega\text{-cm})^{-1}$
D_{Na^+} = 8.083 x 10^{-6} (cm^2/sec)	t_e = 7.055 x 10^{-3}
μ_{Na^+} = 7.996 x 10^{-5} (cm^2/volt-sec)	$t_\oplus$ = 5.76 x 10^{-5}
C_{Na^+} = 0.0294 (mole/cm^3)	D_e = 3.15 x 10^{-3} (cm^2/sec)
	μ_e = 0.031 (cm^2/volt-sec)
	C_e = 5.462 x 10^{-7} (mole/cm^3)

The diffusion coefficient of electrons which are the predominant minor defects in a Na_2SO_4 melt, was determined by the voltage relaxation method suggested by Weiss (49). Its average value is 3.15 ($\pm$0.17) x 10^{-3} cm^2/sec. The corresponding drift mobility of electrons is 0.031 cm^2/volt-sec which is identical to that in Na-NaCl melts ar 1166 K with 0.81 mole percent of sodium.

The effects of Cr_2O_3, Al_2O_3, and SiO_2 on total conductivity as well as the electronic conductivity were examined by the A.C. impedance technique and Wagner-Hebb type polarization experiments. The introduction of Cr_2O_3 at concentration levels of 10^{-3}, 10^{-2}, 10^{-1}, and 1 mole percent has significant effects on the total electrical conductivity i.e., as the amount of Cr_2O_3 in the melt increases the total electrical conductivity decreases. Additionally, the dissolved chromia decreases electron conductivities and increases electron hole conductivities. The addition of Al_2O_3 into the melt does not produce significant changes in total electrical conductivities. However, the Al_2O_3 lowers electron conductivities tremendously and increases electron hole conductivities slightly. The melts containing silica show small changes in total electrical conductivities but massive decrements in electron conductivities.

The oxidation and/or hot corrosion rate is often considered as a product of total conductivity, sum of ionic transport numbers, and the transport number of major electronic species. The results observed in the present investigation indicate the sum of ionic transport numbers is nearly unity; therefore, the product of total conductivity and the transport number of the major electronic species is considered. Such considerations are described in Fig.5 as a function of mole percent of oxides in the melt. The value of total conductivity x transport number of major electronic species for a pure Na_2SO_4 is 1.64×10^{-3}. As indicated in this figure the reaction rate is decreased as a function of mole percent of each oxide in the melt. For Cr_2O_3 and Al_2O_3 melts, it levels off at about 10^{-1} mole percent while SiO_2 melts do not level off even in supersaturated melts. It is clear from this figure that the addition of silica has the utmost effect on decreasing reaction rates among those protective oxides tested.

CONCLUSIONS AND SUMMARY

To obtain the dissolution of the stabilizing components, mass transport in the coating must occur. The presence of point defects in a crystalline solid greatly effect the transport properties in that solid. The nature and concentration of these defects can be altered which, in turn, can impart large changes in the transport properties of a material (eg. ionic conductivity and diffusion). In this study, we are determining the defect structures of yttria and ceria-stabilized zirconium oxides. Using electrical conductivity measurements, the activation energies of yttria-stabilized zirconia have been examined as a function of frequency, composition, and oxygen activity. Conductivity measurements on ceria-stabilized zirconia have shown anomalous results. At low oxygen activities, ZrO_2-CeO_2 samples did not reach equilibrium. The cause for this phenomenon has yet to be determined. However, high temperature x-ray diffraction studies are currently underway to discover the effect of these low oxygen activities on the ZrO_2-CeO_2 structure.

It was observed that the total electrical conductivity of pure Na_2SO_4 was of the order of 2.32×10^{-1} $(ohm\text{-}cm)^{-1}$ and varied only slightly with changes in the activities of Na_2O. The cationic transport number of a pure Na_2SO_4 melt was found to be about 0.984 at 1173 K and was almost a constant as a function of Na_2O. The partial conductivity of electrons in $Na2SO_4$ was about two orders of magnitude less than the total electrical conductivity. Thus, the transport number of electrons, t_e is of the order of 10^{-3} in a pure Na_2SO_4 melt at 1173 K. The self-diffusion coefficient of Na^+ ions was estimated utilizing the above experimental data and its average value was 8.1×10^{-6} cm^2/sec.

The transient relaxation method was employed to determine the diffusion coefficient of electrons in a pure Na_2SO_4 melt and its value was about $3.15 \times 10^{-3} cm^2/sec$ at 1173 K.

The introduction of the protective oxides such as Cr_2O_3, Al_2O_3, and SiO_2 into a Na_2SO_4 melt has significant changes in transport properties of the melt. These oxides decrease the electron conductivities and increase the electron hole conductivities as compared to pure Na_2SO_4.

REFERENCES

1. Bornstein, N. S., Literature Review of Inhibition of Vanadate Attack, ONR N00014-88-M-0013, June 1988

2. Bornstein, N. S. and M.A. DeCrescente, Corrosion, 26, 7, 209-14, July 1988

3. Luthra, K. and D. Shores, A Study of the Mechanism of Hot Corrosion in Environments Containing NaCl, NRL Contract N000173-77-C-0253, Fifth Quarterly Progress Report, November 1978

4. Luthra, K. and D. Shores, A Study of the Mechanism of Hot Corrosion in Environments Containing NaCl, NRL Contract N000173-77-C-0253, Sixth Quarterly Progress Report, February 1979

5. Luthra, K. and D. Shores, A Study of the Mechanism of Hot Corrosion in Environments Containing NaCl, NRL Contract N000173-77-C-0253, Sixth Quarterly Progress Report, May 1979

6. Jones, R. L. and S. Gadomski, J. Electrochem. Soc., 124, 10, 1641-1648, 1977

7. Shores, D., D. McKee, and T. Kerr, Sodium Chloride Induced Hot Corrosion: Literature Survey and Preliminary Experiments, Contract 7A003-CIP105 (EPNHT05), April 1976

8. Jones, R. L., Low Quality Fuel Problems With Advanced Materials, NRL Report 6252, August 1988

9. Luthra, K. and H. Spacil, J. Electrochem. Soc., 129, 3, 649-656, 1982

10. Fitzer, E. and J. Schwab, Corrosion, 12, 49-54, 1956

11. Flood, H. and T. Forland, Acta Chem. Scand., 1, 592, 1947

12. Kingery, W., H. Bowen, and D. Uhlmann, Introduction to Ceramics, 2nd edition, Wiley, New York, 1976, p.125

13. Su, M. Y., Point Defect Structure of Chromium Sesquioxide, PhD thesis, Penn State Univ., 1987, p.4-6

14. Kroger, F. A., Chemistry of Imperfect Crystals, Wiley, New York, 1964, p.194

15. Simkovich, G. and F. F. Aplan, "The Influence of Solid State Imperfections in Mineral and Metal Processing", Metallurgical Processes for the Year 2000 and Beyond, ed. by Sohn, H. Y. and E. S. Geskin, The Mineral, Metals & Materials Society, 1988

16. Simkovich, G. and J. B. Wagner, Jr., J. Electrochem. Soc., 110, 513-516, 1963

17. Nii, K., Corr. Sci., 10, 571-583, 1970

18. Jones, C. F., R. L. Segall, R. St. C. Smart, and P. S. Turner, J. Chem. Soc., Faraday Trans. I., 73, 1710-1720 , 1978

19. Jones, C. F., R. L. Segall, R. St. C. Smart, and P. S. Turner, J. Chem. Soc., Faraday Trans. I., 74, 1615-1624, 1978

20. Jones, C. F., R. L. Segall, R. St. C. Smart, and P. S. Turner, J. Chem. Soc., Faraday Trans. I., 74, 1624-1633 , 1978

21. Illis, A., G. Nowlan, and J. Koehler, CIM Bulletin, 63, 352-361, 1970

22. Lussiez, P. K. Osseo-Asare, and G. Simkovich, Met. Trans., 12B, 651-657, 1981

23. Rogers, G., G. Simkovich, and K. Osseo-Asare, Hydrometallurgy, 10, 313-328, 1983

24. Wan, R. Y., J. D. Miller, and G. Simkovich, "Enhanced Ferric Sulfate Leaching of Cu from $CuFeS_2$ and Carbon Particle Aggregates", Inter. Conf. on Recent Adv. in Min. Sci. and Tech., MINITEK 50, 1984

25. Wagner, C., J. Phys. Chem. Solids, 33, 1051-1059, 1972

26. Beckmann, J. D., A. Birchenall, and G. Simkovich, "Electrical Conductivity of Dispersed Phase Systems", First Inter. Conf. on Transport of Non-Stoichiometric Compounds, ed. by J. Nowotny, Elsevier Sci., New York, 1982, p.8-28

27. Liebert, C., R. Jacobs, S. Stecura, and C. Morse, "Durability of Zirconia Thermal Barrier Coatings on Air Cooled Turbine Blades in Cyclic Jet Engine Operation", NASA TM X-3410, Sept. 1976

28. Sevcik, W. and B. Stoner, "Analytical Study of Thermal Barrier Coated First-stage Blades In a JT9D Engine", NASA CR-135360, Jan. 1977

29. Carlson, N. and B. Stoner, "Study of Thermal Barrier Coatings on High Temperature Industrial Gas Turbine Engines", NASA CR-135147, Feb. 1978

30. Subbarao, E. C., "Zirconia an Overview", Science and Technology of Zirconia, Advances in Ceramics Vol.3, ed, by Heuer, A. H. and L. W. Hobbs, Amer. Cer. Soc., 1981, p. 1-24

31. Wolten, G. W., J. Amer. Cer. Soc., 46, 9, 418-22, 1963

32. Stubican, V. S. and J. R. Hellmann, "Phase Equilibria in Some Zirconia Systems", Science and Technology of Zirconia, Advances in Ceramics Vol.3, ed, by Heuer, A. H. and L. W. Hobbs, Amer. Cer. Soc., 1981, p.25-36

33. Wagner, C., Naturwissenschaften, 31, 265-68, 1943

34. Hund, F., Z. Phys. Chem., 199, 142-51, 1952

35. Tien, T. Y., and E. C. Subbarao, J. Chem. Phys., 39, 4, 1041-47, 1963

36. Etsell, T. H.,and S. N. Flengas, Chem. Rev., 70, 339--76, 1970

37. Takahashi, T., Physics of Electrolytes Vol. 2, ed. by J. Hladik, Academic Press, New York, 1972, p.989-1051

38. Worrell, W. E., Solid Electrolytes, ed. by S. Geller, Springer-Verlag, Berlin, 1977, p.143-168

39. Dell, R. M., and A. Hooper, Solid Electrolytes, ed. by P. Hagenmuller and W. Van Gool , Academic Press, New York, 1978, p.291-312

40. Choudhary, C. B., H. S. Maiti, and E. C. Subbarao, Solid Electrolytes and their Applications, ed. by E. C. Subbarao, Plenum Press, New York, 1980, p.1-80

41. Alcock, C. B., "Transport of Ions and Electrons in Ceramic Oxides", Electromotive Force Measurements in High-temperature Systems, ed. by Alcock, C. B., Institution of Mining and Metallurgy, 1968

42. Patton, J. S. and R. L. Clarke, "Hot Corrosion Resistance of Yttria-Stabilized Zirconia Coatings", 1989 Tri-Service Corrosion Conference, 1989

43. Nagelberg, A. S., J. Electrochem. Soc., 132, 2502, 1985

44. Jones, R. L., and C. E. Williams, J. Electrochem. Soc., 132, 1498, 1985

45. Jones, R. L., and C. E. Williams, J. Electrochem. Soc., 133, 227, 1986

46. Singhal, S. and R. J. Bratton, "Stability of a $ZrO_2(Y_2O_3)$ Thermal Barrier Coating in Turbine Fuel with Contaminant", J. Eng. for Power, 102, 4, 770-775, 1980

47. Palko, J., K. Luthra, and D. McKee, "Evaluation of performance of Thermal Barrier Coatings Under Simulated Industrial/Utility Gas Turbine Conditions", Final Report, General Electric Co., 1978

48. Zaplatynsky, I., "Reactions of Yttria-Stabilized Zirconia with Oxides and Sulfates of Various Elements", DOE/NASA/2593-78/1, NASA TM-78942, 1978

49. Weiss, K., Z. Phys. Chem. (N.F.),59, 242, 1968

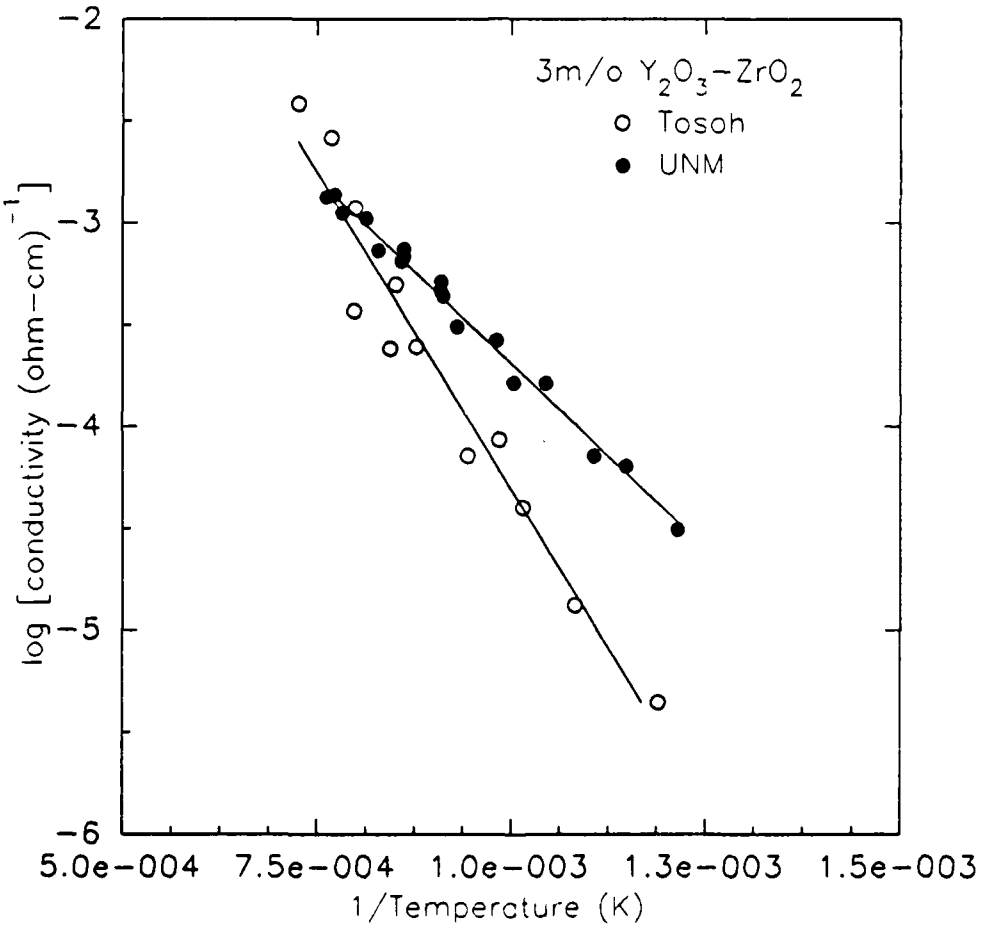

Figure 1 AC conductivity (1khz) vs temperature for two different grain sizes

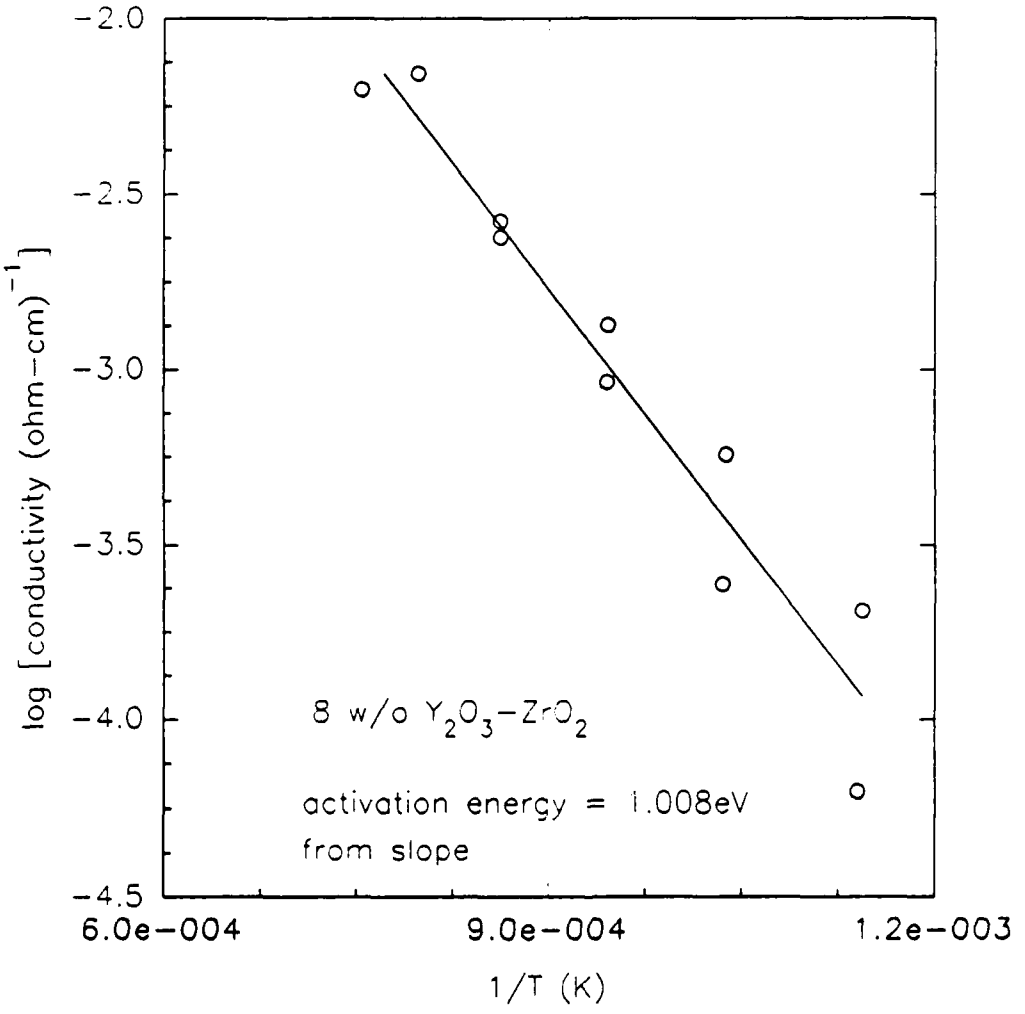

Figure 2 AC conductivity (1khz) for 8wt% Y_2O_3-ZrO_2 as a function of temperature

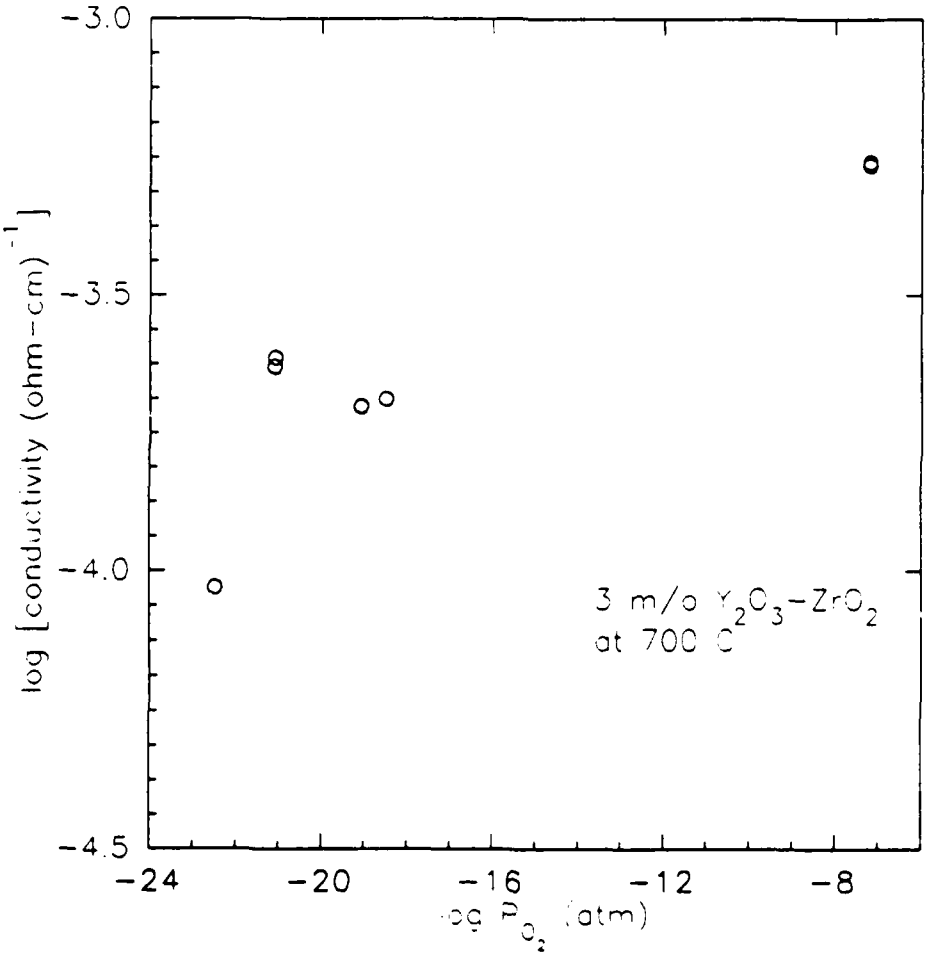

Figure 3 AC conductivity (1khz) for 3 mole% Y_2O_3-ZrO_2 as a function of oxygen partial pressure

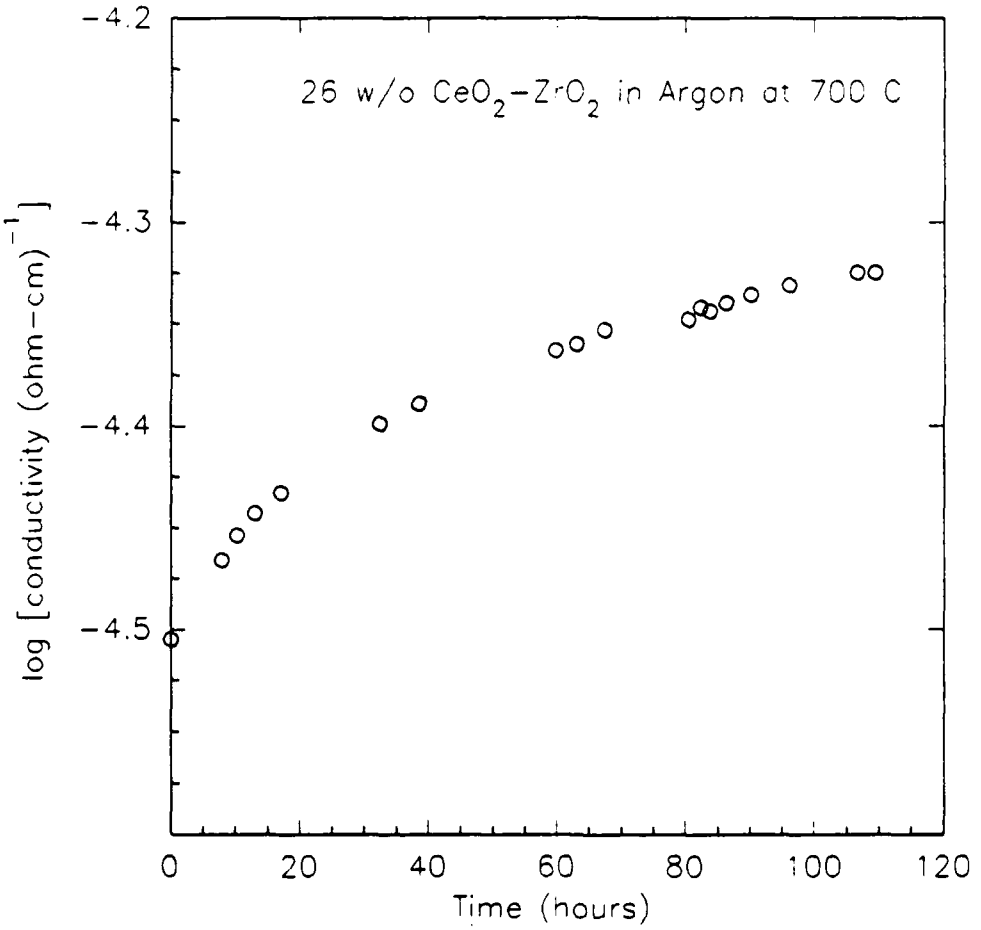

Figure 4 AC conductivity (100hz) vs time for 26wt% CeO_2-ZrO_2 at 700°C

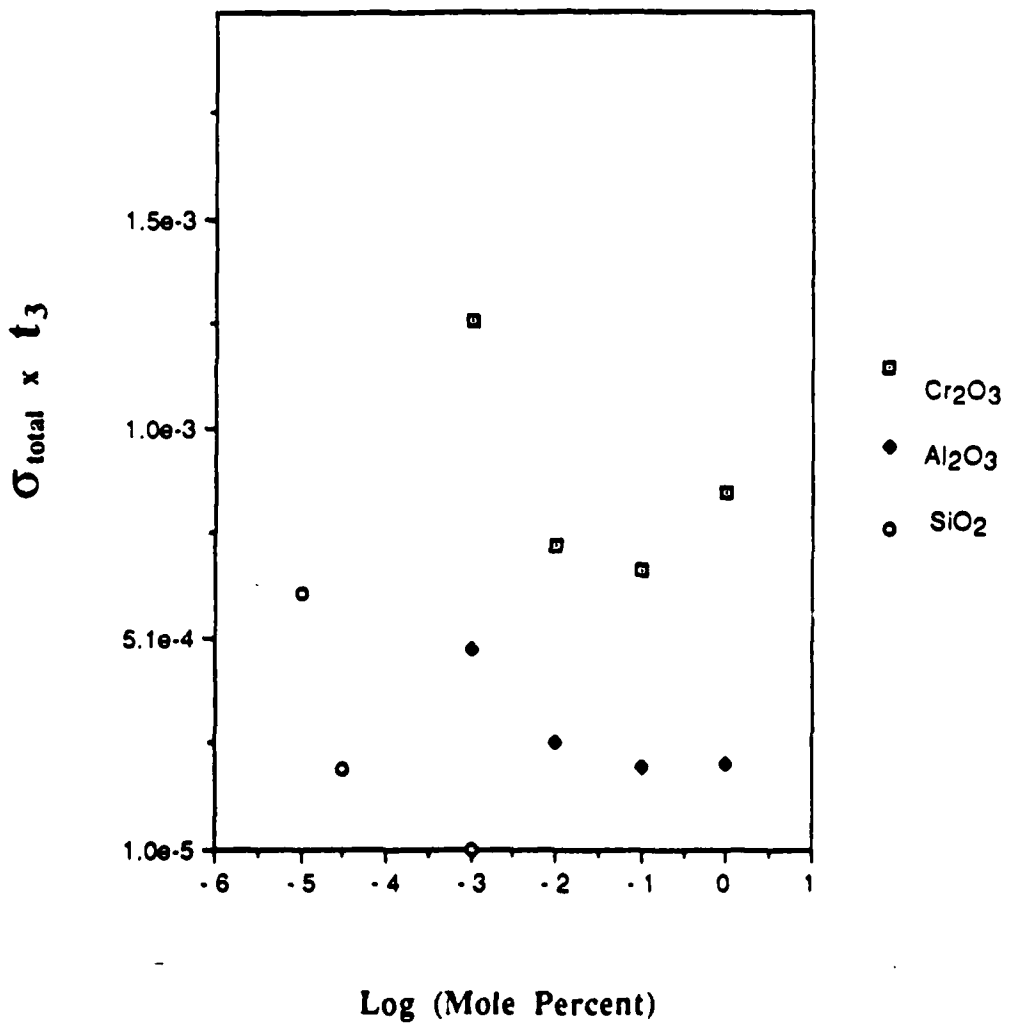

Figure 5 Average value of total conductivity times transport number of electronic species as a function of mole% of oxides added in the melt at 1173 K